

Article

Indoor thermal loss test on small-size solar receiver (UF-RT01) for process heat application

Giacomo Pierucci*, Sahand Hosouli, Michele Salvestroni, Matteo Messeri, Federico Fagioli, Maurizio De Lucia

Department of Industrial Engineering, University of Florence, 50139 Florence, Italy



ARTICLE INFO

Keywords:

Thermal loss
Small-size PTC
UF-RT01
parabolic troughs receiver
Test rig
Experimental analysis

ABSTRACT

The parabolic trough collector is one of the most promising technologies for medium temperature application. The energy of solar radiation is directed by parabolic mirrors into cylindrical receivers and transmitted to a heat transfer fluid. Thus, the characteristics of absorber tubes have a direct influence on overall thermal efficiency of the system. A novel receiver (UF-RT01) for small-size parabolic trough collectors is tested using two coaxial tubes made from stainless-steel with a selective coating, inserted in a glass envelope. In this layout, the fluid inlet and outlet are at the same side. The paper describes the realization of a laboratory test stand for thermal loss measurement of small-size receivers in steady-state condition, based on Joule effect heating supplied by multiple electric resistances. A prototype tube is analyzed experimentally and performances are evaluated as a function of different operating temperatures, reaching up to 180 °C. A maximum value for thermal loss amounts at about 24 W when the receiver average temperature is 180 °C.

1. Introduction

Renewable sources can play an important role in reducing the consumption of fossil fuels. The energy request in industrial application involves a noticeable fraction (more than 30%) of the total requested supply for human activities in developed countries [1]. In general, solar collectors could be used to meet the demand of industrial process heat in the range from 60 to 260 °C [2]. At least, this sector represents the most promising area for this technology [3,4], beyond power application. A novel small-size parabolic trough collector was properly developed to carry out this task.

As yet, the majority of concentrating solar technologies had been limited to large installations in order to produce power [5]. For standard size receivers (absorber tube outer diameter of 70 mm) indoor test stands have been developed at several institutions with the aim of studying thermal loss. The evaluation of the thermal loss can be performed in various modes such as steady-state equilibrium, quasi-steady-state equilibrium and surface temperature measurements [6].

Vernon E. et al. [7], published a comprehensive technical report on SEGS LS-2 solar collector efficiency and thermal losses. The tests were done as a function of the operating temperature for different selective coatings and vacuum level in the receiver annulus. The absorber diameter of SEGS LS-2 receiver was 70 mm and the length was 4 m. The mea-

surements were set up in off-sun mode, i.e. the collector was defocused and the receiver was shaded from direct sunlight. At 180 °C above the ambient temperature, the thermal loss is around 13 W/m with Cermet selective coating.

F. Burkholder et al. [8], from NREL fabricated a test stand to evaluate thermal loss of Solel UVAC2 and Schott PTR70 receivers in steady-state equilibrium condition. In this paper, two coiled cable heaters and one cartridge heater were used. At increasing absorber temperatures, the cartridge heater supplies most of the thermal input to the system. Coil heaters were used for compensating end loss effects and creating an adiabatic boundary. Solel UVAC 2 and Schott PTR70 receivers showed a similar thermal loss value of 370 W/m at operating temperatures of 400 °C.

Another study from NREL on UVAC3 parabolic trough receiver was published as a technical report and UVAC3 parameters results were compared to UVAC2 results. Three internal electric resistance heaters were used in this report. The output values were 310 and 380 W/m at 400 °C, respectively [9]. Two Schott's 2008 PTR70 parabolic trough receivers with 70 mm absorber diameter were also tested on NREL rig with three internal electric resistance heaters including one cartridge heater was fully inserted into the receiver and two outer coil heaters were used in surfaces contact with the interior of the copper pipe (receiver tube). Thermal loss correlation coefficients were derived from laboratory ex-

* Corresponding author.

E-mail addresses: giacomo.pierucci@unifi.it (G. Pierucci), sahand.hosouli@unifi.it (S. Hosouli), michele.salvestroni@unifi.it (M. Salvestroni), matteo.messeri@unifi.it (M. Messeri), federico.fagioli@unifi.it (F. Fagioli), delucia@unifi.it (M. De Lucia).

<https://doi.org/10.1016/j.seja.2021.100010>

Received 9 August 2021; Received in revised form 8 November 2021; Accepted 9 November 2021

Available online 14 November 2021

2667-1131/© 2021 The Authors. Published by Elsevier Ltd. This is an open access article under the CC BY-NC-ND license (<http://creativecommons.org/licenses/by-nc-nd/4.0/>)

Nomenclature

Abbreviations

PTC	Parabolic Trough Collector
TC	Thermocouples
RTD	Thermoresistance sensors

Variables

A	Cross section of the absorber [m^2]
CR	Local concentration ratio [-]
DNI	Direct normal irradiation hitting the collector [W/m^2]
k	Thermal conductivity of the absorber [$\text{W}/(\text{m} \text{ } ^\circ\text{C})$]
I	Supplied current [A]
l	Circumference of the absorber [m]
P_g	Gross power incoming the receiver tube per length unit [W/m]
P_{in}	Supplied power due to Joule effect [W]
Q_{ad}	Conductive power at the absorber's inlet [W]
Q_L	Power from longer cartridge [W]
Q_{loss}	Thermal loss [W]
Q_s	Power from shorter cartridge [W]
U	Supplied voltage [V]
U_l	Thermal loss coefficient [$\text{W}/(\text{m}^2 \text{ } ^\circ\text{C})$]
T_{amb}	Ambient temperature [$^\circ\text{C}$]
T_{Ave}	Average temperature of the receiver [$^\circ\text{C}$]
ΔT	Difference between the average and ambient temperature [$^\circ\text{C}$]
Δx	Distance between the temperature sensors at the absorber's inlet [m]

Greek symbols

α	Absorbance of the receiver's coating [-]
γ	Intercept factor [-]
ρ	Mirror's reflectance [-]
τ	Glass envelope transmittance [-]

periments. The thermal loss value at an average absorber temperature of $320 \text{ } ^\circ\text{C}$ above ambient temperature was $140 \text{ W}/\text{m}$ [10].

J. M. Márquez et al. [11], from PSA (Plataforma Solar de Almería), introduced a new test bench called HEATREC to study the receiver tubes in a chamber with vacuum and atmospheric pressure conditions. Eight internal electric resistances of $\sim 6.3 \text{ } \Omega/\text{m}$ were used as heaters. These heaters were connected to two electrical power supplies. In order to counteract the edge effect resulted in temperature drop in the absorber ends, two additional small electrical heaters of $\sim 750 \text{ } \Omega$ were inserted at the end of the receiver. The thermal loss value at $360 \text{ } ^\circ\text{C}$ average absorber temperature above the ambient temperature for vacuum and atmospheric pressure condition inside the test chamber was 220 and $227 \text{ W}/\text{m}$, respectively.

S. Dreyer et al. [12] from DLR reported a test rig in order to investigate the behavior of a receiver comparing the results with the thermal loss predictions from optical measurements. For an absorber with an emissivity of 7%, 9.3% and 11.4% at $400 \text{ } ^\circ\text{C}$, the thermal loss values were about 189 , 237 and $272 \text{ W}/\text{m}$, respectively. G. Hoste and N. Schuknecht from SkyFuel studied thermal efficiency of parabolic trough receiver for large-aperture collector, based on Joule effect heating in a steady-state condition. In this setup, an electrical current was run through the receiver to heat the absorber's material resistively [13].

J. Pernpeintner et al. [14], studied systematic temperature deviations due to overheating by the cartridge heaters. This study presents the measurement of absorber temperature over-prediction as function of heating power and the results showed that absorber temperature over-prediction is at a relevant order of magnitude for thermal loss measurements of parabolic trough receivers (with 70 mm absorber). Also M. Sanchez et al. [15] from CENER reported a testing facility for the

measurement of optical and thermal properties of receivers: the stand uses two electrical heating to reach the desired operating temperatures consisting of an electrical resistance with 2 m length and two end coil electrical heaters with 3 cm width.

Another study from J. Pernpeintner et al. [16] reported a method to measure the optical efficiency of an assembled evacuated receiver using a steady-state method in an indoor solar simulator. This study from DLR in QUARZ Center reported two test benches for the measurement of the specific heat loss at operating temperature and the optical efficiency. For optical efficiency test based on increase of enthalpy, the receiver is irradiated with solar simulator lamps in the ELLIREC test bench. However, test results from this optical test bench do not provide an absolute value and a standard reference test sample has been introduced.

CF. Kutscher and J. C. Netter [17] from NREL presented a new outdoor thermal transient test method for measuring the optical efficiency with potentially high accuracy of evacuated receivers in parabolic trough solar collectors. In this study, water and aluminum shot have been used as thermal mass inside the receiver tube. Results from this study (based on proposed method) are in match with the true wavelength spectrum of the receiver in actual operational condition. Inserted aluminum tube inside the stainless-steel absorber tube showed significantly better results. R. López-Martín et al. [18], developed an outdoor test bench to measure the optical efficiency of solar receiver tubes under real solar radiation conditions. This study described the test procedure and performance evaluation for two receiver tubes from a European and Asian manufacturer. Similar to previously mentioned studies [16,17], optical efficiency is measured by transient method based on a simplified energy balance. This study showed that the results were similar at various ambient temperatures and at different times of the year.

Furthermore, a technical specification document has been published on general requirements and test methods for solar receivers by International Electrotechnical Commission (IEC). IEC TS 62862-3-3:2020 includes the characterization and definitions of performance parameters, geometry, technical properties and the test methods for optical characterization, heat loss, and durability of solar thermal receivers for absorbing concentrated solar radiation [19].

As mentioned before, all the cited studies are referred to standard receivers for parabolic trough collectors. In order to spread the technology beyond power generation sector, for industrial purpose and heat production (at medium temperature), such systems need be revised toward a scale down process. Plants with mirrors of $5\text{--}6 \text{ m}$ are indeed not feasible for the integration in urban context and new, compact, modular solutions and layouts have to be set up. The Department of Industrial Engineering of Florence University developed a small size concentrating collector described in [20]. It was designed from an optical, thermal, structural point of view through different physical models [21] and some prototypes were built. Many measurement campaigns have been carried out to test the single parts and verify the expected performance of the system. Because of the reduction of the components' dimensions, experimental methods and facilities need to be adapted and improved, especially for the small size absorbers. Sensor's layout, such as heating suppliers positioning, have to be configured properly due to the lack of space, reaching a reliable measure without affecting thermal phenomena.

In this context, a test rig has been realized at Department of Industrial Engineering of Florence University for evaluating the thermal performance of small size solar receivers (in the specific case the absorber tube diameter is 10 mm). This paper describes the test procedure and thermal loss test results on a prototype at steady-state condition with the implementation of an internal heating process due a proper electrical cartridge. A previous study had been conducted in the same laboratory with slightly different test rig and receiver [22].

In that case a copper bar, insulated by a dielectric sleeve, was inserted inside the absorber forming a continuous electrical circuit with the absorber itself (made by copper) and the Joule effect is given by a direct current applied on it. Only one thermocouple could be used for

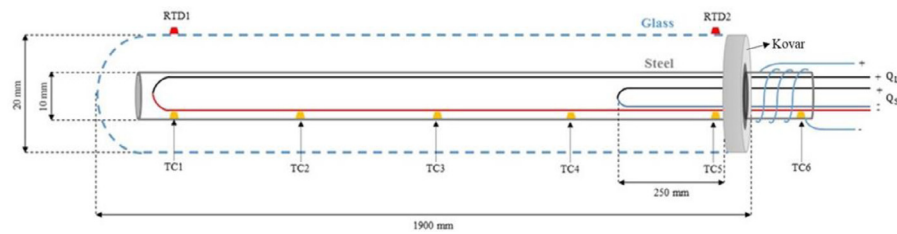


Fig. 1. Scheme of the One-End receiver tube for m-PTC and the set-up layout.

monitoring the internal temperature due to the limitations in space. Furthermore, some assembling criticalities arise in the electrical contact between the copper bar and the absorber that was not accessible; the local resistance could vary, introducing the possibility of non-uniform thermal power supply. The results in the previous configuration had shown that the maximum thermal loss was 23.5 W at internal temperature of 180 °C.

2. Experimental apparatus and procedure

2.1. Small size absorber tube

The receiver tube is a key component of parabolic trough collectors. The one considered in this study is UF-RT01 (University of Florence – Receiver Tube 01) receiver tube and has been designed and developed by our research group. The tube has a specific design, being formed by two coaxial tubes so that the fluid inlet and output are at the same side. It was properly developed to scale the PTC technology toward smaller size (chord length from 6–8 m to around 0.5 m): the purpose is the installation in urban context and the application in industrial process. The outer absorber tube is made of stainless-steel and has a diameter of 10 mm (1 mm thickness) for a length of 1860 mm; the smaller coaxial tube is made of stainless-steel and has an internal diameter of 6 mm (0.5 mm thickness). Furthermore, a selective coating (Cermet coating, $\alpha=0.94$ for $\lambda < 2.5 \mu\text{m}$ and $\varepsilon=0.13$ for $\lambda > 2.5 \mu\text{m}$ at ambient temperature) has been selected to reduce the emission in infrared range and increase the energy absorption in solar spectral range. The absorber tube is covered by a glass envelope made of standard borosilicate without anti-reflective (AR) layer. Inside, a vacuum level is fixed at 10^{-4} mbar to reduce the thermal losses to the radiative ones. In order to keep the absorber tube aligned in the reflector focus, four springs support are inserted. A small cylinder of Kovar is used as a junction between metal and glass tubes (on the right side of Fig. 1). This is to compensate the different thermal expansion coefficients of the two materials and to avoid the glass break. The stainless-steel outlet tube is then welded on a plug. In respect to standard PTCs technology, the proposed small size receiver is meant to be applied in collectors suitable for roofs or compact installation areas. The chord length is therefore limited under 500 mm and the absorber diameter could not be directly scaled down from the standard one to avoid too small flow section surface and high-pressure loss. The diameter is then set at 10 mm. This led to obtain a concentration ratio of about 13 (aperture length/absorber circumference), lower than in the standard PTC. Consequently, thermal loss is expected to be higher per unit aperture area. At the same time, the one side inlet/outlet configuration is considered advantageous because it helps in piping layout and in ensuring the internal vacuum condition over time (the glass envelope is indeed sealed itself one side).

2.2. Test rig set-up

The thermal loss measurement is set up under indoor test without Sun irradiance, imposing a controlled internal heating. This process is based on the Joule effect, feeding electric heaters with current to obtain a steady state condition at different reference temperatures. By removing the inner coaxial stainless-steel tube, a cartridge heater (Q_c) is

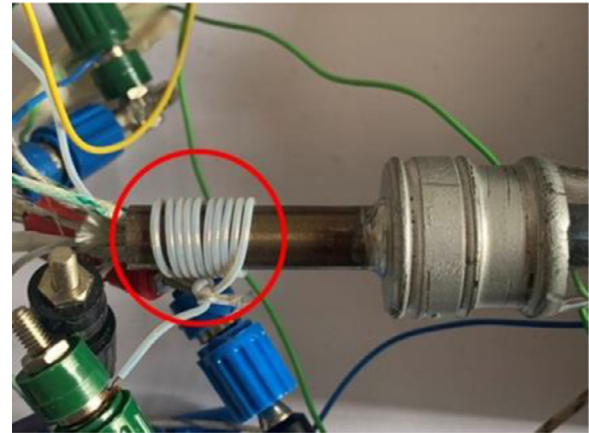


Fig. 2. External heater.

inserted along the length of absorber tube (Fig. 1). In order to increase the uniformity of temperature along the tube and to eliminate the axial temperature gradient, a second shorter cartridge heater (Q_c) is placed inside with a length of 250 mm from the outlet section of receiver tube. An additional external heater (Fig. 2) is placed before the Kovar part to meet the adiabatic condition, minimizing the temperature gradient between the portion of the metallic tube which is covered by glass and the one that stands in air. The cartridges are made of a nickel-chrome wire (electrical resistance of 5 Ω/m) covered by polymeric shield and they are fed with three different direct supply up to 30 Vs.

Six thermocouples are used to measure the temperature along the absorber (Type T with accuracy of ± 1 °C). TC1-TC5 are placed uniformly along the tube (fixed to the heater to slide inside the tube Fig. 3a); TC6 is positioned outside to check the temperature gradient along the outlet section. Furthermore, the temperature of the glass envelope is evaluated by the placement of two 1/3 DIN class RTDs at the beginning and at the end of tube: Fig. 3b shows their placement on glass. Another RTD monitors the ambient temperature. Fig. 4 shows an overall schematic of the experimental apparatus.

3. Test procedure and experimental results

The measurement chain was completed connecting the sensors to a data acquisition unit. It has been programmed to manage data reading and recording processes. A customized graphical user-interface has been developed properly with Labview Software and used for real time monitoring.

In order to achieve a desired uniform temperature along the receiver tube, some preliminary test should be conducted on the heating supplier parameters. However, the size of tube could not permit to check the precise position of sensors and the real surface contact among them, the heaters and the absorber tube.

Once the heating devices are placed in the test stand, electrical supply is increased step by step for all of them separately, until reaching steady-state condition at different temperature levels. This procedure is a slow process, taking also hours, in which every change causes an un-

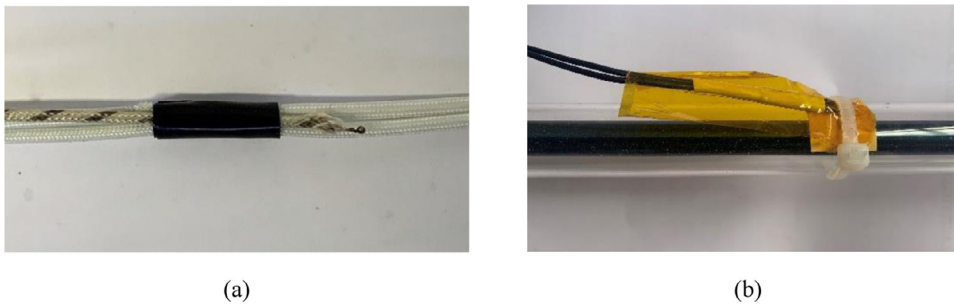


Fig. 3. (a) TC placement on the heater inside the absorber, (b) RTD placement on the glass tube of receiver.

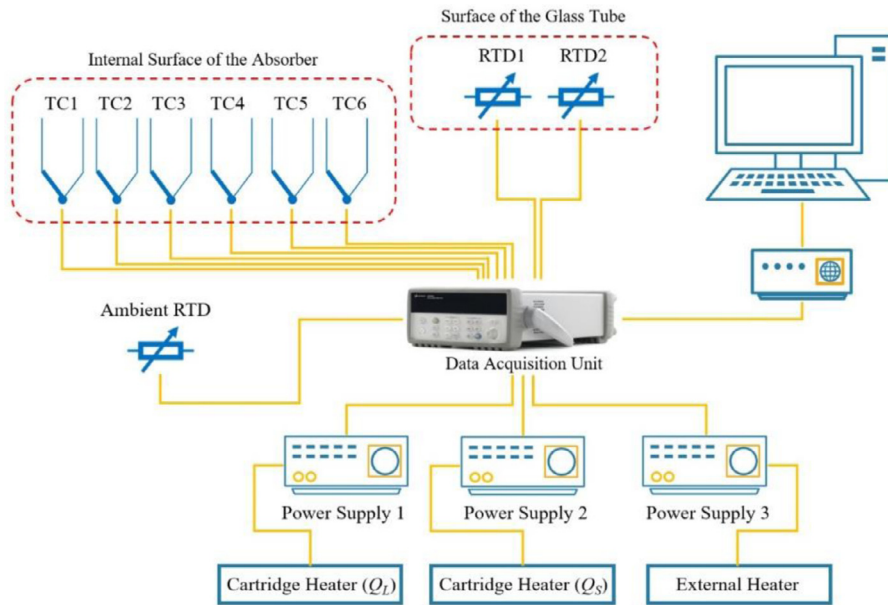


Fig. 4. Schematic of the experimental apparatus.

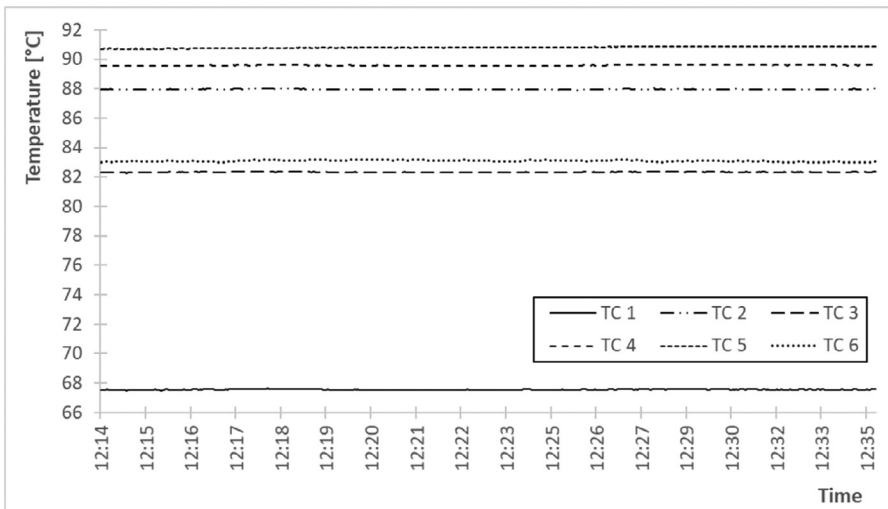


Fig. 5. Temperature variation along the absorber tube in Test 9.

balancing of the temperature gradient along the tube. The input power P_{in} due to Joule effect is derived thanks to voltage (U [V]) and current (I [A]) for each heater with Eqn 1:

$$P_{in} = V \cdot I \text{ [W]} \quad (1)$$

The test procedure was repeated for 28 cases in the range of interest. For instance, in test 9, an average temperature of 88 °C was reached along the tube and Fig. 5 shows that the temperature stability was kept for over 20 min under the uncertainty of thermocouples. Furthermore,

the maximum temperature difference is limited at 9 °C with the exception of the final part of the receiver tube (TC1) which got colder than 23 °C in respect to the higher value.

For the other tests, the equilibrium temperature increased with higher electrical power, finding similar behavior of the rig. Table 1 shows temperature variation along the receiver tube among the 28 tests at stable conditions in addition to the electric power of heaters. In this table, ΔT is the difference between average absorber temperature and ambient temperature.

Table 1
Test parameters and temperature variation along the receiver tube.

Test	Q_L Power [W]	Q_S Power [W]	Total Power [W]	TC1 [°C]	TC2 [°C]	TC3 [°C]	TC4 [°C]	TC5 [°C]	TC6 [°C]	$(T_{Avr}-T_{amb})$ [°C]
1	0.346	0.076	0.422	32	33	32	33	34	33	13
2	0.379	0.066	0.445	31	32	32	33	34	32	12
3	0.832	0.062	0.894	34	41	39	40	41	40	20
4	0.832	0.060	0.893	35	40	39	40	41	40	20
5	2.195	0.112	2.307	48	60	57	61	60	59	40
6	2.195	0.112	2.307	48	59	57	60	60	59	39
7	2.998	0.140	3.139	52	67	64	67	67	66	47
8	2.997	0.140	3.138	53	67	64	68	67	66	47
9	4.977	1.001	5.978	68	88	82	90	91	83	70
10	4.927	0.414	5.340	68	88	82	88	91	82	67
11	4.925	0.489	5.414	68	88	83	89	91	83	67
12	5.887	0.523	6.409	83	108	105	107	105	106	86
13	8.262	0.491	8.753	86	116	106	117	117	116	93
14	8.261	0.491	8.752	86	116	106	117	117	116	93
15	9.167	0.459	9.626	88	122	111	122	120	120	98
16	9.169	0.458	9.627	88	122	111	123	121	120	98
17	9.999	1.659	11.658	94	128	115	129	128	128	106
18	11.252	0.458	11.710	96	136	122	136	130	130	110
19	13.331	0.701	14.032	105	147	131	148	144	144	122
20	13.329	0.700	14.029	105	147	148	148	144	144	126
21	17.720	1.308	19.030	119	169	148	170	169	168	143
22	17.718	1.284	19.002	119	169	148	170	170	168	143
23	18.444	1.725	20.170	123	171	151	173	174	173	147
24	18.439	1.718	20.158	123	171	151	173	174	171	146
25	19.939	1.213	21.151	125	177	155	179	169	169	149
26	19.905	1.226	21.132	125	177	155	179	169	168	150
27	20.834	1.513	22.347	125	182	158	183	182	182	155
28	21.529	2.686	24.215	128	183	159	185	192	166	161

The overall evaluation and comparison of recorded data showed that TC1 values are never in match with the others. This is mainly attributable to a displacement of the thermocouple in the end of tube. The lack in the contact between Q_L heater and the tube is less probable: they have a similar diameter and the tolerance is small while inserting the heating device. In any case, it is not possible to verify the real internal configuration because there is no access in that side of the absorber. For these reasons, the authors decided to calculate and report thermal loss for a reference average temperature T_{ave} excluding TC1 values. TC6 was also not taken into account since it is not under vacuum conditions (it is in contact with the outlet part of the tube beyond the Kovar cylinder).

It is also important to remark that test need a very long time (at least 5 h for low power) to get stable conditions and a small increment/decrement in the power supply for one of the heaters causes a non-negligible but slow change in the temperature distribution. In these operating settings, a maximum standard deviation of 14.3 °C was accepted for the highest average temperature (test 28 at 180 °C) while, for lower values such as 40, 59, 88, 106, 119, 143, 164 and 176 °C it drops down to 0.8, 1.6, 3.7, 1.7, 5.5, 7.8, 10.7 and 12.2 °C, respectively. A specific constraint was fixed as necessary condition: time intervals were chosen for processing data only when each temperature resulted constant with a variation inside sensor's accuracy (± 1 °C). The stable part of test lasted more than 1:30 h on average.

Then thermal loss could be derived thanks to Eq. 2:

$$Q_{loss} = Q_L + Q_S - Q_{ad} \text{ [W]} \quad (2)$$

$$Q_{ad} = \frac{kA}{\Delta x} (TC5 - TC6) \text{ [W]} \quad (3)$$

Where Q_S and Q_L are the heater power supplying the absorber, k is the thermal conductivity of stainless-steel, A is the stainless-steel pipe cross-section area, TC5 and TC6 are temperature values and Δx is the distance between them. The parameters k , A and Δx are 13 W/(m °C), 28.27 mm² and 40 mm, respectively. Therefore, again, Eq. (3) represents the conductive dissipation (or contribute depending on the sign of the temperature difference) through the absorber section area at the tube outlet (Q_{ad}). Despite of the controlled heating device showed in Fig. 2,

the gradient between TC5 and TC6 was not completely zeroed during test.

4. Results and discussions

The measurement set-up lets to find the correlation between thermal loss and average temperature for a solar receiver in the range of interest (up to about 180 °C). Since among 28 tests many of them are related to the same interval, the temperatures along the absorber tube during the campaign is summarized for 8 tests (Fig. 6). Excluding TC1, the reference stable temperature is 40, 59, 88, 106, 119, 143, 164, 167, 176 °C in ascending order. For each value, the equilibrium supply power for heaters (Q_S and Q_L) were evaluated and the same amount of power is assumed to be dissipated to the external ambient mainly due to irradiation process (vacuum between absorber and glass limits convection and conduction phenomena). In the outlet part of the tube, another contribution for heat transfer arises where the stainless-steel joints Kovar and creates a thermal bridge. It should be reduced as much as possible in order to characterize the intrinsic properties of the absorber tube (for instance the coatings emissivity in a future modeling activity). With this purpose, the third heater was implemented and regulated, to avoid a significant temperature gradient from the external edge to the metal part covered by glass.

In Fig. 7 and Table 2, the evaluated thermal loss power is reported as a function of the difference between average absorber temperature and ambient temperature (ΔT). A maximum value of 23.98 W is found when ΔT is 161 °C (tube average temperature of 180 °C). The fitting quadratic curve was derived through Matlab and results Eq. (4), with a correlation coefficient up to 0.994 and a root-mean-square deviation of 0.2%:

$$Q_{loss} = 9.107 \cdot 10^{-4} \Delta T^2 + 3.870 \cdot 10^{-3} \Delta T \text{ [W]} \quad (4)$$

Consequently, the thermal loss coefficient U_l could be given per square meter of the steel absorber surface as a function of the same ΔT (Eqn 5:

$$U_l = 3.206 \cdot 10^{-6} \Delta T^2 + 1.191 \cdot 10^{-2} \Delta T + 5.066 \cdot 10^{-1} \left[\text{W}/(\text{m}^2 \text{ °C}) \right] \quad (5)$$

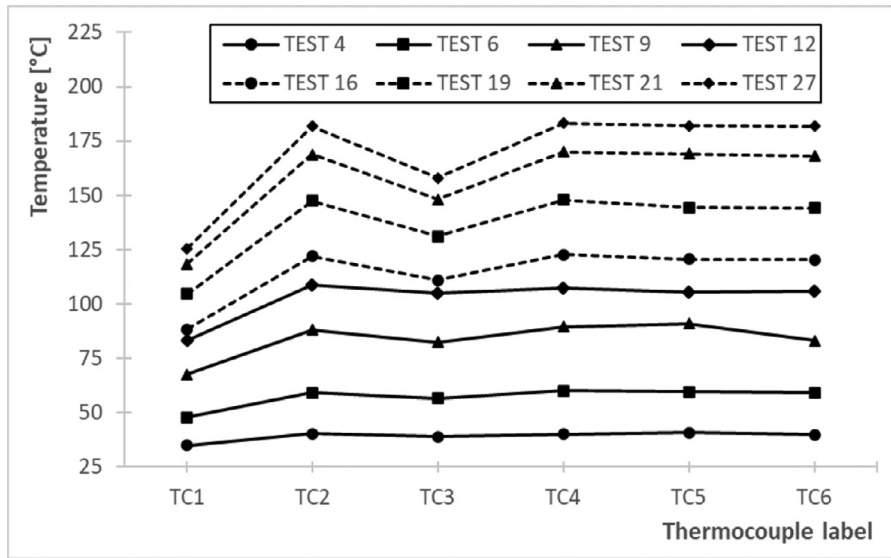


Fig. 6. Temperatures distribution along the absorber tube during main tests.

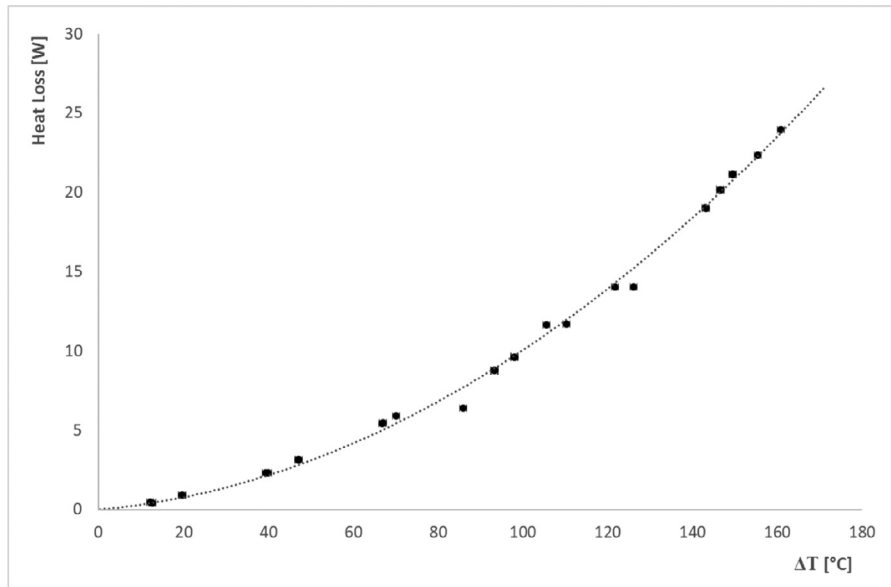


Fig. 7. Thermal loss as a function of the difference between the average absorber temperature and the ambient temperature.

Table 2
Test values for temperatures and thermal loss with errors.

Test	T_{ave} [°C]	ΔT [°C]	ΔT error [°C]	Q_{loss} [W]	Q_{loss} error [W]	Test	T_{ave} [°C]	ΔT [°C]	ΔT error [°C]	Q_{loss} [W]	Q_{loss} error [W]
1	33	12.7	0.8	0.4352	0.0009	15	119	97.9	0.8	9.6288	0.0007
2	33	12.1	0.8	0.4589	0.0002	16	119	98.1	0.8	9.6289	0.0007
3	40	19.6	0.8	0.9003	0.0003	17	125	105.6	0.8	11.6571	0.0012
4	40	19.8	0.8	0.90018	0.00011	18	131	110.3	0.8	11.7103	0.0009
5	59	40.0	0.8	2.3107	0.0002	19	143	121.8	0.8	14.0333	0.0009
6	59	39.5	0.8	2.3110	0.0002	20	147	126.1	0.8	14.0309	0.0009
7	66	47.1	0.8	3.1452	0.0003	21	164	143.1	0.8	19.039	0.002
8	66	47.3	0.8	3.1455	0.0003	22	164	143.2	0.8	19.0167	0.0013
9	88	70.1	0.8	5.9070	0.0007	23	167	146.7	0.8	20.1839	0.0013
10	88	66.9	0.8	5.424	0.007	24	167	146.5	0.8	20.1854	0.0014
11	88	67.0	0.8	5.4872	0.0004	25	170	149.4	0.8	21.154	0.004
12	106	85.9	0.8	6.415	0.019	26	170	149.6	0.8	21.142	0.013
13	114	93.2	0.8	8.7661	0.0006	27	176	155.5	0.8	22.3472	0.0015
14	114	93.5	0.8	8.7657	0.0007	28	180	160.9	0.8	23.978	0.004

At the maximum tested difference of temperature (operative to environment, 160.9 °C) U_l reached 2.55 W/(m² °C). The correlation coefficient arose 0.984 with a root-mean-square deviation of 0.4%.

Uncertainty is evaluated for all the measured values taking into account Type A errors for experimental data measurement and Type B errors for instrument characteristics and equipment uncertainty [23]. Combined standard uncertainty is used for error propagation in the derived parameters, based on the sum-of-the-squares method [24]. The reported expanded uncertainty is based on a standard uncertainty multiplied by a coverage factor $k = 2$, providing a level of confidence of approximately 95%. For instance, the error u_{loss} associated to thermal power could be calculated with Eq. 6:

$$u_{loss} = \sqrt{\left(\frac{\partial Q_{loss}}{\partial Q_S} u_S\right)^2 + \left(\frac{\partial Q_{loss}}{\partial Q_L} u_L\right)^2 + \left(\frac{\partial Q_{loss}}{\partial Q_{ad}} u_{ad}\right)^2} \quad (5)$$

where u_S , u_L , u_{ad} are the errors related to the different heating contributes. The total uncertainty values for the thermal loss in tests are in the order of mW. For temperature difference, the necessity to use thermocouples bring a maximum absolute error of 0.8 °C. Considering the measurement span, relative mean error stands around 0.04% for thermal loss and 1.5% for temperature.

As mentioned before, the UF-RT01 was developed aiming at scaling solar concentrating technology towards small dimension to integrate them in urban context. Some considerations could arise in the comparison with receivers for standard PTC systems. In the market two tubes have been selected as a reference for UF-RT01 even the application is different such as working conditions and purpose (Schott and Archimede Solar Energy). In order to address the issue of space limitation in urban-industrial areas, UF-RT01 has been developed with much lower diameter (10 mm compared as 70 mm of the commercial absorbers [25,26]).

Table 3, indicates the design parameters of above-mentioned receiver tubes. The thermal loss of SCHOTT, Archimede and UF-RT01 receiver tubes at 130 °C (difference between operating conditions and ambient temperature) are 5.75, 9.30 and 8.28 W/m, respectively.

By considering the mentioned receiver tubes in a solar system unit with a length of 1 m (in similarity with the other geometric dimensions), the incoming power could be evaluated imposing the following boundary conditions:

- Direct normal irradiation DNI of 800 W/m²;
- local concentration ratio [19] CR of 13.1 (indicative value for small systems);
- intercept factor γ of 0.96 [27];
- reflectance of mirrors ρ equal to 0.92 (for polymeric film reflectors).

In this context other external variables which are related to the overall system layout such as the incidence angle modifier, shading, end loss and cleanliness factors are neglected (fixed at 1). Consequently, the peak gross power comes P_g in 1 m tube [W/m] (Eq. 6):

$$P_g = DNI \cdot CR \cdot l \cdot \rho \cdot \gamma \cdot \tau \cdot \alpha \quad (6)$$

where l is the circumference of the absorber. The product between CR and l represents the aperture segment for the collected Sun power in the reference concentrator system (the analysis is carried out per length unit). In relation to the specific diameter, the SCHOTT, Archimede and UF-RT01 systems receive 1861, 1861 and 245 W/m as a gross value, respectively.

On one hand, with modules in similarity at 130 °C (difference between operative and ambient temperature), almost eight meters of UF-RT01 receiver are required to gain a comparable amount of net power from one meter of the commercial tubes, including heat loss which were directly deduced by the performance curve in the datasheet of products [25,26]. In detail, 1855, 1852 W comes out from SCHOTT, Archimede while eight meters of UF-RT01s get 1895 W.

On the other hand,

Table 4 is reporting the reliable cost per meter of the different technologies. For the reference length, the lower performance of UF-RT01s

Table 3
Design parameters of solar systems with UF-RT01 and two receiver tubes available in the market (Schott and Archimede Solar Energy) and thermal properties at ΔT equal to 130 °C.

Receiver	Diameter [mm]	Absorbance [-]	Glass transmittance [-]	Specific heat loss [W/m]	CR [-]	Gross Power [W]	Relative heat loss [%]	Specific Cost [€/m]
SCHOTT	70	0.95	0.966	5.7	13.1	1861	0.3%	400
Archimede	70	0.95	0.966	9.3	13.1	1861	0.5%	400
UF-RT01	10	0.92	0.92	8.3	13.1	245	3.4%	30

Table 4
Receiver's reference length, collector's width and cost for configurations with similar net thermal power.

Receiver	Reference receiver's length [m]	CR [-]	Reference collector's width	Net Power [W]	Cost [€]
SCHOTT	1	13.1	2.88	1855	400
Archimede	1	13.1	2.88	1852	400
UF-RT01	8	13.1	0.41	1895	240

is compensated by a much lower specific cost per meter. Then, the UF-RT01 receiver layout results the 60% cheaper than commercial solutions at the same collected power.

5. Conclusion

A test rig for small-size solar receivers (UF-RT01) have been realized and a specific prototype has been tested in order to evaluate the thermal loss. The dimensions of the absorber force to adapt the procedures on literature with a specific attention for sensors choice and positioning as well as for power supply devices. Since the thermal loss are expected to be low (under 50 W), simple wire heaters could be implemented, managing small values of current (under 1 A) and voltages. That allows high accuracy in measurement even if the experiments run for hours to reach stability and changing boundary conditions is slow (many hours).

The results on the tested prototype show the behavior of its performance at increasing temperature up to 180 °C. In that regime a maximum thermal loss of 23.98 W is found while at lower fixed temperatures (40, 59, 88, 106, 119, 143, 164 and 176 °C) it drops down to 0.9, 2.31, 5.91, 6.41, 9.63, 14.03, 19.03 and 22.35 W, respectively.

Mentioned laboratory thermal loss test stand will be a useful tool for evaluating the current and future small-size receivers for parabolic trough collectors. By now, the work will be also focused on outdoor testing of thermal loss for comparison and confirmation of results.

A preliminary cost evaluation was carried out to underline the potential of the scale down process about concentrating solar systems. The development and realization of the UFR01 receiver demonstrated that small sizes are not necessarily related to higher cost such as it is quite usual in advanced technologies. In this case, even accepting a drop in the thermal performance the designed absorber system results to be convenient and promising.

Author contributions

Conceptualization and methodology, G.P., S.H., M.S., M.M., F.F., M.D.L.; writing-original draft preparation, G.P and S.H.; writing-review & editing, G.P., S.H. and M.D.L.; supervision and project administration, M.D.L.

Declaration of Competing Interests

The authors declare that they have no known competing financial interests or personal relationships that could have appeared to influence the work reported in this paper.

Acknowledgments

The work reported here represents the joint efforts of many individuals in the research group of Prof. M. De Lucia in the Department of Industrial Engineering of Florence (DIEF). The current research received funding from the "PON 2014-2020 Ricerca e Innovazione" program (under FSE) through the SOLARGRID project with grant agreement n° ARS01_00532. The authors would also like to thank Luciano Albanelli, Luca Foronchi and Leonardo Baldi from University of Florence for useful help and discussion during the project.

References

- [1] G. Coccia, G. Di Nicola, A. Hidalgo, *Parabolic Trough Collector Prototypes For Low-Temperature Process Heat*, Springer, 2016 ISBN 3319270842.
- [2] S. Kalogirou, The potential of solar industrial process heat applications, *Appl. Energy* 76 (2003) 337–361.
- [3] G. Böllük, M. Mert, Fossil & renewable energy consumption, GHGs (greenhouse gases) and economic growth: evidence from a panel of EU (European Union) countries, *Energy* 74 (2014) 439–446.
- [4] C. Lauterbach, B. Schmitt, U. Jordan, K. Vajen, Potential for solar process heat in Germany-Suitable Industrial sectors and processes, *Proc. Eurosun Graz, Österreich* (2010).
- [5] W. Fuqiang, C. Ziming, T. Jianyu, Y. Yuan, S. Yong, L. Linhua, Progress in concentrated solar power technology with parabolic trough collector system: a comprehensive review, *Renew. Sustain. Energy Rev.* 79 (2017) 1314–1328.
- [6] E. Lüpfert, K.-J. Riffelmann, H. Price, F. Burkholder, T. Moss, Experimental analysis of overall thermal properties of parabolic trough receivers, *J. Sol. Energy Eng.* (2008) 130.
- [7] V.E. Dudley, G.J. Kolb, A.R. Mahoney, T.R. Mancini, C.W. Matthews, M. Sloan, D. Kearney, Test results: SEGS LS-2 Solar Collector, Sandia National Labs, Albuquerque, NM United States, 1994.
- [8] F. Burkholder, M. Brandemuehl, H. Price, J. Netter, C. Kutscher, E. Wolfrum, Parabolic trough receiver thermal testing, in: *Proceedings of the ASME 2007 Energy Sustainability Conference; American Society of Mechanical Engineers Digital Collection*, 2007, pp. 961–970.
- [9] F. Burkholder, C. Kutscher, Heat-loss Testing of Solel's UVAC3 Parabolic Trough Receiver, National Renewable Energy Lab.(NREL), Golden, CO United States, 2008.
- [10] F. Burkholder, C. Kutscher, Heat Loss Testing of Schott's 2008 PTR70 Parabolic Trough Receiver, National Renewable Energy Lab.(NREL), Golden, CO United States, 2009.
- [11] J.M. Márquez, R. López-Martín, L. Valenzuela, E. Zarza, Test bench HEATREC for heat loss measurement on solar receiver tubes, in: *Proceedings of the AIP Conference Proceedings*, 1734, AIP Publishing LLC, 2016, p. 30025.
- [12] S. Dreyer, P. Eichel, T. Gnaedig, Z. Hacker, S. Janker, T. Kuckelkorn, K. Silmy, J. Pernpeintner, E. Luepfert, Heat loss measurements on parabolic trough receivers. 16th SolarPACES, Perpignan, Fr (2010) 8.
- [13] G. Hoste, N. Schuknecht, Thermal efficiency analysis of SkyFuel's advanced, large-aperture, parabolic trough collector, *Energy Procedia* 69 (2015) 96–105.
- [14] J. Pernpeintner, B. Schiricke, Parabolic trough receiver heat loss measurement–Correction of absorber temperature over-prediction, in: *Proceedings of the AIP Conference Proceedings*, AIP Publishing LLC, 2019 Vol. 2126.
- [15] M. Sanchez, E. Mateu, D. Perez, P. García, F. Villuendas, C. Heras, R. Alonso, Optical and thermal characterization of solar receivers for parabolic trough collectors, *Pro. Adv. Sci. Technol.; Trans. Tech. Publ.* 74 (2010) 313–319.
- [16] Meyen, S.; Lüpfert, E.; Pernpeintner, J.; Fend, T. Optical characterisation of reflector material for concentrating solar power technology. 2009.
- [17] C.F. Kutscher, J.C. Netter, A method for measuring the optical efficiency of evacuated receivers, *J. Sol. Energy Eng.* (2014) 136.
- [18] R. López-Martín, L. Valenzuela, Optical efficiency measurement of solar receiver tubes: a testbed and case studies. *Case Stud, Therm. Eng.* 12 (2018) 414–422.
- [19] IEC Solar thermal electric plants - Part 3-3: systems and components - General requirements and test methods for solar receivers; 2020;
- [20] G. Pierucci, S. Hosouli, M. Messeri, M. Salvestroni, F. Fagioli, F. Taddei, A. Pourreza, H. Rashidi, M. De Lucia, Realization of a test rig for small solar collectors and preliminary test, in: *Proceedings of the AIP Conference Proceedings*, AIP Publishing LLC, 2019 Vol. 2126.
- [21] M. Salvestroni, G. Pierucci, F. Fagioli, A. Pourreza, M. Messeri, F. Taddei, S. Hosouli, H. Rashidi, M. De Lucia, Design of a small size PTC: computational model for the receiver tube and validation with heat loss test, in: *Proceedings of the IOP Conference Series: Materials Science and Engineering*, 556, IOP Publishing, 2019, p. 12025.
- [22] G. Pierucci, S. Hosouli, M. Salvestroni, M. Messeri, F. Fagioli, F. Taddei, M. De Lucia, Experimental Methodology and Thermal Loss Tests on Small Size Absorber Tubes for Solar Applications, *Energies* 11 (2018) 2552.
- [23] N. Janotte, E. Lüpfert, R. Pitz-Paal, K. Pottler, M. Eck, E. Zarza, K.-J. Riffelmann, Influence of measurement equipment on the uncertainty of performance data from test loops for concentrating solar collectors, *J. Sol. Energy Eng.* (2010) 132.
- [24] Dieck, R.H. Measurement uncertainty: methods and applications; ISA, 2007; ISBN 1556179154.
- [25] SCHOTT PTR®70 Receiver Tube Available online: http://www.schott.com/d/csp/370a8801-3271-4b2a-a3e6-c0b5c78b01ae/1.0/schott_ptr70_4th_generation_brocure.pdf.
- [26] Archimede Solarenergy Receiver Tube Available online: <http://www.archimedesolarenergy.it/download.htm>.
- [27] S. Ulmer, K. Pottler, E. Lu' pfer, Ro' ger, M. Measurement techniques for the optical quality assessment of parabolic trough collector fields in commercial solar power plants, *Proc. Energy Sustain.* 47977 (2007) 1085–1091.